

Magnesium Doped Titania for Photocatalytic Degradation of Dyes in Visible Light

Balaram Kiran Avasarala^{1*}, Siva Rao Tirukkovalluri² and Sreedhar Bojja³

¹Department of Chemistry, Jazan University, Jazan, Kingdom of Saudi Arabia

²Department of Inorganic and Analytical Chemistry, Andhra University, Visakhapatnam, India

³Inorganic and Physical Chemistry Division, Indian Institute of Chemical Technology, Hyderabad, India

Abstract

Magnesium doped titanium dioxide ($\text{Mg}^{2+}\text{-TiO}_2$) with varying magnesium weight percentages (0.25 - 1.0 wt.%) has been synthesized by sol-gel method and is characterized by XRD, UV-Visible, XPS, SEM and FT-IR methods. XRD data has shown anatase crystalline phase in $\text{Mg}^{2+}\text{-TiO}_2$ catalysts indicating that Mg^{2+} did not influence the crystal patterns of TiO_2 . Absorption shift due to the presence of Mg^{2+} ions in the TiO_2 structure is significant. SEM image revealed that doped catalyst has smaller particle size and higher surface area than undoped TiO_2 . FT-IR spectral study along with XPS established the substitution of Mg^{2+} into TiO_2 lattice. The photocatalytic efficiency of the synthesized catalysts was investigated by performing photocatalytic degradation of methyl orange dye (MO) under visible light irradiation and it has been found that the $\text{Mg}^{2+}\text{-TiO}_2$ catalysts possess better catalytic activity than undoped TiO_2 . The effect of dopant concentration, pH, catalyst, dosage and pollutant concentrations was studied for obtaining optimal degradation conditions.

Keywords: Magnesium; Titania; Sol-gel method; Doping; Photocatalysis

Introduction

Problems related to waste water remediation have emerged as a high national and international priority. Effluents discharged from industries contain toxic organic and inorganic chemicals, which need to be treated prior to disposal. Waste waters generated by the textile industry are rated as the most polluting among all industrial sectors, considering both the volume rejected and the composition of the effluents [1]. It contain large amount of azo-dyes which are also used in the industry of paper making, pharmacy, textile, cosmetics and food processing. Owing to their nature, these effluents constitute a major threat to the surrounding ecosystem [2]. The increased public concern with these environmental pollutants and the stringent international environmental standards have prompted the need to develop novel treatment methods for converting such dye-containing effluents, into harmless compounds [3,4].

Being mostly non-biodegradable under both natural and sewage treatment plant conditions, these dyes like methyl orange, poses special environmental concern due to their toxicity and potential carcinogenic nature [3,5]. Acute exposure to methyl orange will cause health problems such as increased heart rate, vomiting, cyanosis and tissue necrosis in humans. Conventional methods for the treatment of these chemicals are limited by: economic reasons, oxidative potential, effluent characteristics, resistance to aerobic degradation or tendency to form harmful disinfectant by-products, leading to the transfer of pollutants from the aqueous phase to other, without their destruction [6].

In recent years, there is a growing interest in the use of semiconductors as photosensitizers for the complete oxidative mineralization of pollutants by oxygen [7], pointing out its potential prominent role in the wastewater purification. There are a lot of different semiconducting materials which are readily available but only a few are suitable for sensitizing the photomineralization of a wide range of organic pollutants. TiO_2 , ZnO , Fe_2O_3 , CdS and ZnS are various semiconducting photocatalysts, among which TiO_2 is one of the most suitable semiconducting materials in different media [8,9]. As it is proficient of decomposing a wide range of organic and inorganic pollutants and toxic materials [8,10]. The main polymorphs of TiO_2 , rutile and anatase, are commonly used in photocatalysis, with anatase

showing a higher photocatalytic activity [11-13]. Anatase higher activity is usually attributed to its larger specific surface area.

Though TiO_2 is superior to other semiconductors for many practical uses, the following two types of defects limit its photocatalytic activity [14,15]:

i) Because of its high band gap (3.2 eV), TiO_2 is active only under UV light ($\lambda < 380$ nm) which is only 4-5% of the overall solar spectrum. This restricts the use of sunlight or visible light.

ii) The high rate of electron-hole recombination in TiO_2 particles results in low photoquantum efficiency.

To overcome these limitations of TiO_2 number of strategies have been proposed among which, doping of selective metal ions into TiO_2 is significant [16-18]. The advantage behind doping the metal ions into TiO_2 is the temporary trapping of the photogenerated charge carriers by the dopant and the inhibition of their recombination during migration from inside of the material to the surface [16]. Many researchers have used transition metal ions [18], alkaline metals [16], Zn^{+2} [19], Fe^{+3} [20], Ag, Au, Pd, Pt [21], Li, Rb [22] to improve the photocatalytic activity of TiO_2 . Karakitsou and Verykios [23] showed that doping with cations having valency higher than +4 can increase the photoactivity whereas Mu et al. [24] reported that doping with trivalent or pentavalent metal ions was detrimental to the photo activity even in the UV region.

The properties and photocatalytic activity of a photocatalyst is greatly influenced by the preparation methods. Previous workers have

***Corresponding author:** Balaram Kiran Avasarala, Department of Chemistry, Jazan University, Jazan, Kingdom of Saudi Arabia, Tel: 9868398132; E-mail: drbalaramkiran@gmail.com

Received February 01, 2016; **Accepted** February 29, 2016; **Published** March 03, 2016

Citation: Avasarala BK, Tirukkovalluri ST, Bojja S (2016) Magnesium Doped Titania for Photocatalytic Degradation of Dyes in Visible Light. J Environ Anal Toxicol 6: 358. doi:10.4172/2161-0525.1000358

Copyright: © 2016 Avasarala BK, et al. This is an open-access article distributed under the terms of the Creative Commons Attribution License, which permits unrestricted use, distribution, and reproduction in any medium, provided the original author and source are credited.

developed numerous techniques for fine TiO₂ powders preparation which include vapor decomposition [25], hydrolysis [26], hydrothermal treatment [27], hydrolysis [28], oxidation [29], hydrothermal oxidation [30], mechanical alloying [31], co-precipitation [32] and impregnation [16,21] and sol-gel method [22,33,34].

Sol-gel process is one of the versatile methods to prepare nano-size materials, in contrast to conventional mixed oxide preparation techniques which do not usually produce homogeneous, high surface-area materials. The main advantage of the sol-gel method is its excellent control over the properties of the product via a host of parameters that are accessible in all four key processing steps: formation of a gel, aging, drying and heat treatment. The incorporation of an active metal in the sol during the gelation stage allows the metal to have a direct interaction with support, therefore the material possess special catalytic properties [35].

A study of doping with metal ion having nearly equivalent atomic radius (magnesium), compared to titanium, may give a better insight into doping process in detail and the effect of dopant size on photocatalytic activity. Hence, in the present investigation, the author has adopted a sol-gel method for preparation of magnesium doped TiO₂ and a detailed study has been carried out on its characterization. Evaluation of photocatalytic activity of synthesized catalysts have been carried out by degradation of a representative azo-dye pollutant, methyl orange dye (MO), and also its influence on the photocatalytic degradation of pollutants with environmental concern.

Materials and Methods

Preparation of photocatalysts

Titanium tetra-n-butoxide [Ti(O-Bu)₄], magnesium nitrate obtained from E. Merck (Germany), AR analytical grade, were used as titanium, and magnesium sources for preparing pure TiO₂ (anatase form) and Mg²⁺-TiO₂ photocatalysts. All other chemicals and reagents are of Merck (India) analytical grade.

Initially 21.0 ml of titanium tetra-butoxide was dissolved in 80.0 ml absolute ethanol (100%) and the resulting solution was stirred vigorously. Then 2.0 ml of water and 0.5 ml of acetic acid (50%) were added to another 80.0 ml of ethanol to make an ethanol-water-acetic acid solution. The latter solution was slowly added to the Ti(O-Bu)₄-ethanol solution under vigorous stirring. When the resulting mixture turned to sol, the magnesium nitrate solution (0.25, 0.5, 0.75 and 1.0 wt.%) was added drop-wise.

The resulting transparent colloidal suspension was stirred for more than 2 hours and aged at 25°C until the formation of gel. The gel was dried at 70°C in vacuo at a pressure of 600 psi and then ground. The resulting powder was calcined at 400°C for 2 hours in 50°C increments for every 30 minutes until reaching 400°C. After calcination period, the furnace was allowed to cool for 2 hours. The calcined powders were crushed using an agate mortar and pestle under similar conditions in attempt to produce powders with similar 'fineness' and particle size distributions.

A pure undoped TiO₂ (anatase) sample was also prepared by adopting the above procedure without adding the metal nitrate and is subsequently referred to as pure TiO₂. The doping concentrations are expressed as weight percentage. The powders are stored in black coated air-tight glass containers and were used for XRD analysis, UV-visible absorption studies, XPS, SEM, FT-IR studies and for photocatalytic activity evaluation.

Characterization of photocatalyst

The crystal phase composition of the prepared photocatalysts (TiO₂, Mg²⁺-TiO₂) was determined by X-ray diffraction measurement carried out at room temperature using a PANanalytical, D/Max-III A diffraction with CuK_α radiation (λ=0.15148 nm) with a liquid nitrogen gas-cooled germanium solid-state detector. The accelerating voltage of 35 kV and emission current of 30 mA were used and studied in the range of 2° – 60° 2θ with a step time of 2° min⁻¹. To study the valance state of the photocatalysts, X-ray photoelectron spectroscopy (XPS) was recorded with the PHI quantum ESCA microprobe system, using the AlK_α line of a 250 W X-ray tube as a radiation source with the energy of 1486.6 eV, 16 mA × 12.5 kV, and a working pressure lower than 1 × 10⁻⁸ Nm⁻². As an internal reference for the absolute binding energies, the C 1s peak of hydrocarbon contamination was used as reference to 284.8 eV. The fitting of XPS curves were analyzed with MultiPak 6.0A software. UV-visible absorption spectra were recorded using a Shimadzu UV-2101 spectrophotometer, to study the optical absorption properties of the photocatalyst. The spectra were recorded at room temperature in the wavelength range of 200-800 nm enabling to understand the spectral properties of metal-doped TiO₂ catalysts. The infrared spectra of the synthesized samples are recorded on Thermo-Nicolet Nexus 670 spectrometer, with resolution of 4 cm⁻¹ in KBr pellets. The morphology and size of particles was characterized using SEM (JSM-6610LV) spectrophotometer operated at 20kV.

Photocatalytic activity of catalyst

The photocatalytic efficiency of the synthesized pure and doped TiO₂ catalysts has been evaluated by the degradation of an azo-dye, methyl orange (MO). MO was selected because of well-defined optical absorption characteristics and it can be easily adsorbed onto catalysts from its aqueous solution. Different concentrations (0.1 to 1.1 g) of catalysts were suspended in 100 ml of MO aqueous solution (1.0 to 100.0 mg) in a 150 ml Pyrex glass vessel under rapid stirring using a magnetic stirrer.

The quantitative determination of MO was performed by measuring the absorption of solution at 464 nm with Milton Roy Spectronic 1201, UV-vis spectrophotometer. The extent of MO photodegradation was calculated using a calibrated relationship between the measured absorbance and its concentration. MO cannot be photodegraded in the absence of catalyst under the same irradiation conditions.

The percentage of degradation of MO was calculated from the following equation:

$$\text{Degradation\%} = [1 - A_t/A_0] \times 100$$

Where A_t is the absorbance at time t and A₀ is the initial absorbance of MO before degradation.

Construction of photocatalytic reactor

A photoreactor system is used to accomplish the photocatalytic degradation of methyl orange dye in the presence of visible light, using the doped and undoped TiO₂ photocatalysts. The required amount of catalyst was suspended in 100 ml of standard aqueous solution in a 150 ml Pyrex glass vessel with constant stirring, for uniform illumination of all the catalyst particles.

Running water is passed through the next container continuously to cool the reaction solution and to filter the IR fraction of the light as well as any irradiation below 300 nm [36]. Owing to the continuous cooling, the temperature of the reaction solution is maintained at

approximately $30 \pm 1^\circ\text{C}$. The catalysts were agitated along with dye solution for 45 mins in the absence of light to attain the adsorption/desorption equilibrium on the catalyst surface.

The suspensions were then irradiated under visible light (wavelength range 400 – 800 nm) using a UV filtered Osram high pressure mercury vapour lamp with power 400W and 35000 lumen. The IR (>700nm) and UV (<360 nm) lights were filtered by water and UV filters, respectively. The distance between the light and the reaction vessel was 20 cm. At regular intervals, 5 ml of the aliquots were taken by 0.45 μm Millipore syringe filter and transferred into quartz cuvette for absorbance measurements.

Results and Discussions

Characterization

X-ray diffraction studies: The crystalline phases of the synthesized pure TiO_2 and $\text{Mg}^{+2}\text{-TiO}_2$ were examined by XRD and the diffractograms are given in Figure 1a-1e. The XRD patterns of TiO_2 and all other samples of $\text{Mg}^{+2}\text{-TiO}_2$ (Mg/Ti = 0.25, 0.5, 0.75 and 1.0 wt.%) calcined at 400°C shows only anatase form [37], indicating that Mg^{+2} ions in TiO_2 did not influence the crystal patterns of TiO_2 particle, peaks corresponding to $\text{Mg}(\text{NO}_3)_2$, MgCO_3 and MgO are not detected. The d-spacing and hkl values at different 2θ are recorded and presented.

Since Mg^{+2} is more electropositive, the electronic cloud in each TiO_2 might be loosely held, favoring the formation of less dense anatase phase. In other words, the tight packing arrangement required for rutile phase formation is fully suppressed by the addition of magnesium

nitrate in water which enhances the polarity of water, thus facilitating the formation of anatase phase exclusively. The presence of residual alkyl groups can also reduce the rate of crystallization of TiO_2 which favored the formation of less dense anatase phase [38]. The acetate anion adsorbed on the surface of TiO_2 could also suppress the growth of TiO_2 particles. This type of complexation of acetate anion on the surface of anatase form of TiO_2 may be responsible for the decrease in the crystallite size of TiO_2 in the sol-gel synthesis. Titanium dioxide in the anatase form is the most photoactive and the most practical of the semiconductors for wide spread environmental applications [39,40]. The XRD patterns of all the percentages of $\text{Mg}^{+2}\text{-TiO}_2$ did not show any MgO peaks which indicated that Mg^{+2} ion may be introduced into TiO_2 crystal lattice substitutionally.

Based on the trial photocatalytic degradation patterns of different pollutants with $\text{Mg}^{+2}\text{-TiO}_2$, samples have shown less catalytic activity except 1.0 wt.% $\text{Mg}^{+2}\text{-TiO}_2$. Hence, further characterization have been made only for 1.0 wt.% $\text{Mg}^{+2}\text{-TiO}_2$, which is having intense anatase phase formation and better photocatalytic activity.

UV-Visible Absorption Study: Comparative UV-visible absorption spectra of doped and pure TiO_2 samples are given in Figure 2. The Figure illustrates that there is a shift in the absorption spectra of doped TiO_2 towards visible region (430 nm).

The absorption spectrum of pure TiO_2 consists of a single and broad intense absorption band below 400 nm due to charge-transfer from the valence band (mainly formed by 2p orbitals of the oxide anions) to the conduction band (mainly formed by 3d t_{2g} orbitals of the Ti^{+4} cations)

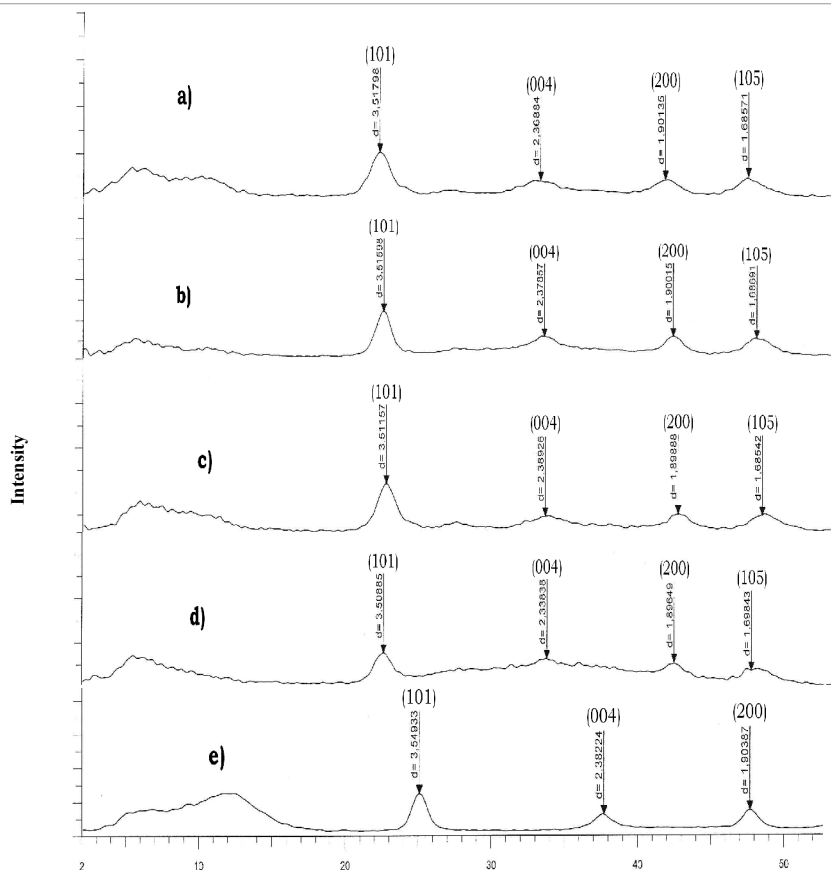


Figure 1: XRD patterns of a) 1.0, b) 0.75, c) 0.5, d) 0.25 wt.% of $\text{Mg}^{+2}\text{-TiO}_2$ and e) Pure TiO_2 heat treated at 400°C for 2 hrs.

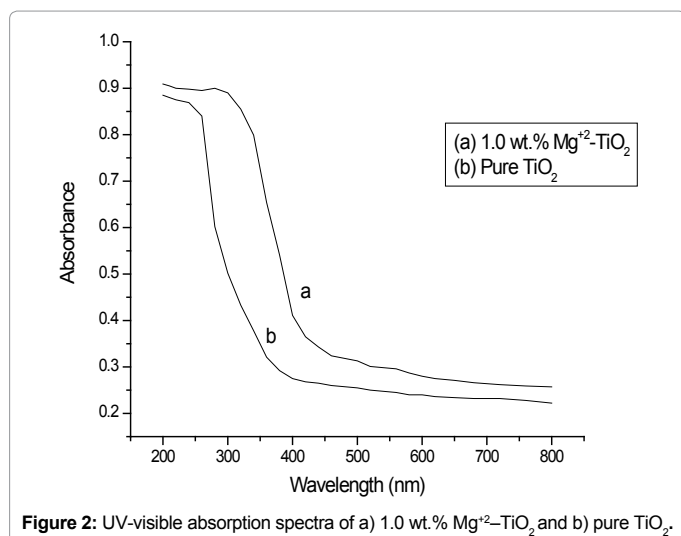


Figure 2: UV-visible absorption spectra of a) 1.0 wt.% Mg²⁺-TiO₂ and b) pure TiO₂.

[41]. But in the doped TiO₂ absorption shifted to higher wavelength region of 400-550 nm. The absorption shift is due to the reduced band gap, with the energy band assumed to be between the top of Mg²⁺ 3s band and the bottom of the Ti⁴⁺ 3d band. Thus the absorption spectra extend to longer wavelengths.

Ray Photoelectron Spectroscopic Study: The XPS analysis was carried out for pure TiO₂ and 1.0 wt.% of Mg²⁺-TiO₂ to determine the chemical composition and the recorded spectra was given in Figure 3a and 3b. In both the spectra, the Ti 2p peaks are narrow with slight asymmetry and have binding energies of 458.63 eV and 464.013 eV, attributable to Ti 2p_{3/2} and Ti 2p_{1/2}. These values are consistent with those reported for titanium in TiO₂ [42,43]. For the 1.0 wt.% Mg²⁺-TiO₂, a binding energy of 51.21 eV (FWHM = 2.675) was observed for Mg_{2p}, which is typical of Mg²⁺ that bonds with oxygen atom [43]. The binding energy was less than that of TiO₂. There wasn't any fitting peak of Ti³⁺ for the 1.0wt.% Mg²⁺-TiO₂. The O 1s peak can be resolved into two peaks, one peak at 528.9 eV and the other at 530.6 eV.

The experimental results of XPS concluded that the entry of Mg²⁺ ion into TiO₂ lattice is substitutional. It is further evidenced by the reports of Serpone and Lawless [44], that the metal dopants are conveniently substituted into the TiO₂ lattice if their ionic radii are identical or nearly identical to that of the Ti (IV) cation. The ionic radius [45] of Mg²⁺ is 0.72Å which is 19.2% larger than Ti⁴⁺ (0.605Å). This clearly indicated that Mg²⁺ is introduced into TiO₂ lattice as substitutional dopant.

Scanning electron microscopic study

The SEM images of TiO₂ and Mg²⁺-TiO₂ catalysts are shown in Figure 4a and 4b. The SEM image of samples containing 1.0 wt.% Mg²⁺ ion show the morphological changes induced by the addition of alkaline earth metal cation. The catalysts are found to contain irregular particle shape which is again aggregates of tiny crystals. Figure 4a shows anatase SEM image of pure TiO₂ which appears as large blocks of coarse material of average particle size 3.8 μm. Figure 4b shows sample containing 1.0 wt.% Mg²⁺, which shows similar features to Figure 4a, with change in the average particle size of 1.04 μm range. This clearly illustrates the altered size and morphology of the catalyst powders and enhanced photocatalytic activity, due to increase in surface area of the catalyst.

FT-IR Spectral Study

FT-IR spectra of pure TiO₂ and 1.0 wt.% Mg²⁺-TiO₂ given in Figure 5a and 5b, have shown peaks corresponding to stretching vibrations of O-H and bending vibrations of adsorbed water molecules around 3380 cm⁻¹ and 1620-1625 cm⁻¹ respectively. Also, a peak was observed around 2900 cm⁻¹, which might be attributable to C-H vibrations likely due to acetate methyl groups.

The broad band below 1200 cm⁻¹ is due to Ti-O-Ti vibration. A peak has been observed at 1065cm⁻¹ which can be assigned to Ti-O-Mg vibration. Hence the FT-IR spectral study along with XPS established the clear substitution of Mg²⁺ into TiO₂ lattice.

Photocatalytic degradation of methyl orange dye (MO)

To evaluate the photocatalytic activity of the Mg²⁺-TiO₂ catalysts, degradation of methyl orange dye (MO) has been carried out under the visible light irradiation in the presence and absence of catalysts. The percentage of MO degradation under visible light is significantly less in the absence of catalyst, whether it is pure or doped TiO₂ (2.95% for 9 hours irradiation). A blank experiment performed in the absence of light along with catalysts demonstrated that no significant change in the MO concentration was observed. To obtain optimum conditions for efficient photocatalytic degradation of MO, various experimental parameters such as catalyst dosage, initial concentration of pollutant and pH are studied by varying each parameter while keeping the others constant.

Effect of dopant concentration on MO degradation

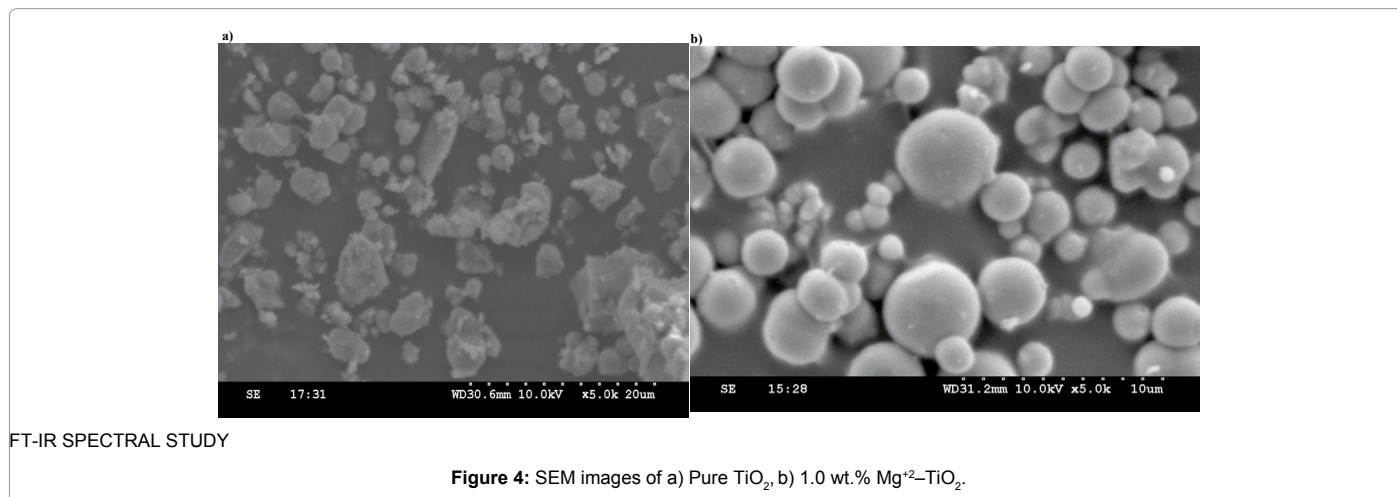
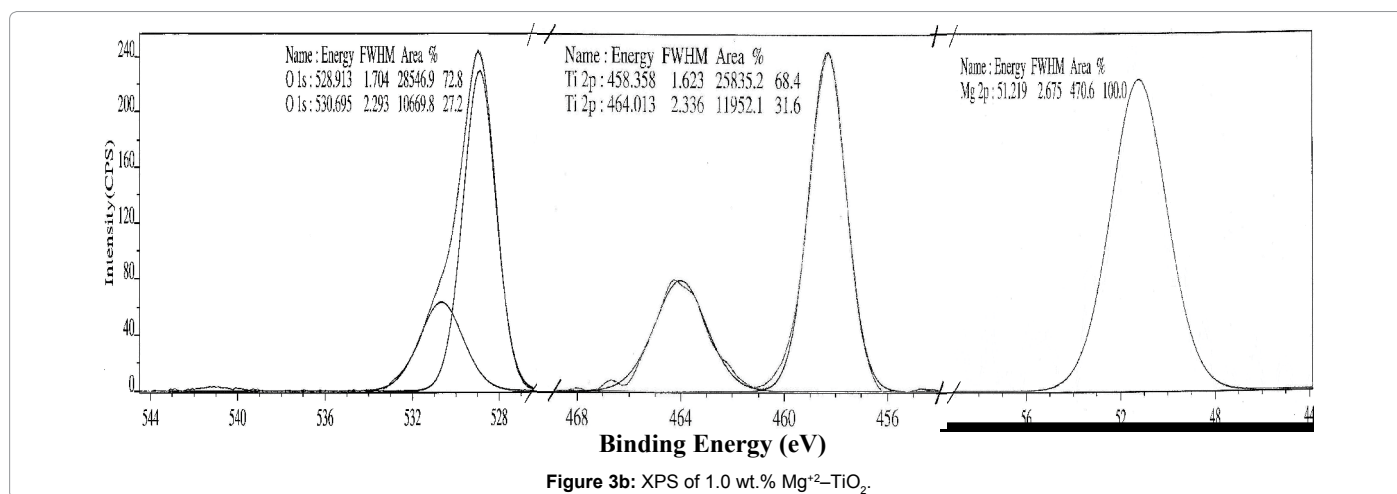
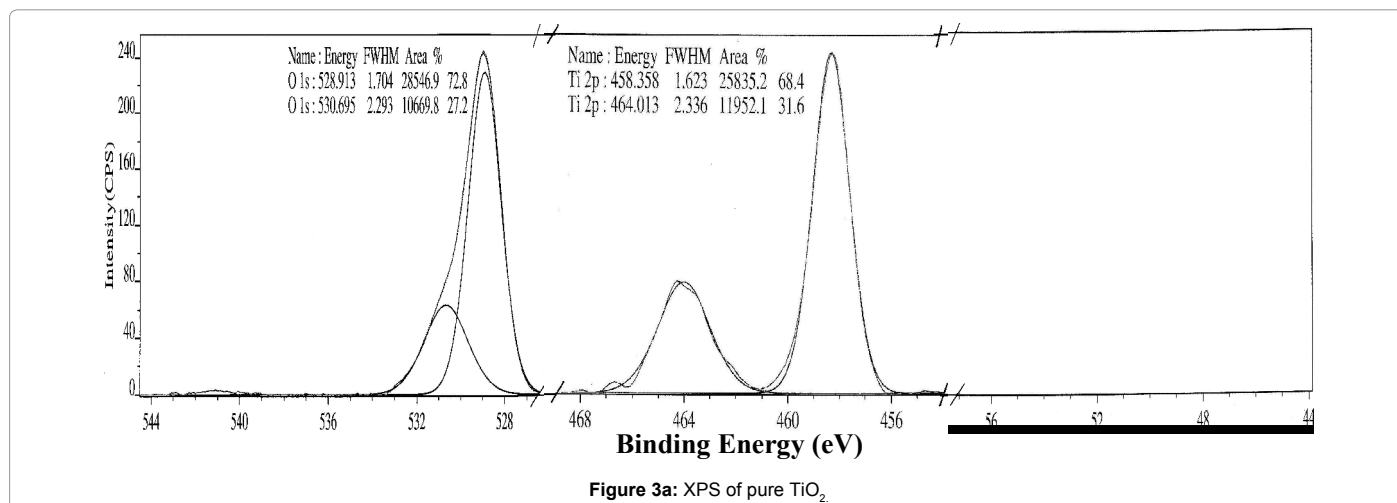
In order to determine the photocatalytic efficiency of Mg²⁺-TiO₂ and to find out an optimum dopant concentration (Mg²⁺), for photocatalytic degradation of MO solution, a set of experiments were carried out using 0.25, 0.5, 0.75 and 1.0 wt.% Mg²⁺-TiO₂ and pure TiO₂. The residual methyl orange concentrations, corresponding to different irradiation time intervals, were quantified by the absorption studies and the results are shown in Figure 6. The results show that as the doping of magnesium ions increase the photocatalytic activity increases up to 1.0 wt.%. Further, increase in magnesium ions doping became detrimental.

The experimental results also revealed that the Mg²⁺ dopant had a significant role in the enhancement of photocatalytic activity of TiO₂. The entry of Mg²⁺ ions may suppress the particle growth and consequently increase in light absorption of TiO₂, which minimize the electron-hole recombination. It also demonstrates that even though the concentration of the doped magnesium ions is small, it still gives much influence on the photocatalytic activity of TiO₂ particles.

Effect of pH

Since, solution pH influences the adsorption and desorption of the substrate, catalyst surface charge, oxidation potential of the valence band and other physico-chemical properties, the catalyst assisted photodegradation of MO has been monitored by in situ measurements of pH of the aqueous suspension with irradiation time, at a fixed weight of catalyst and MO dye concentration at different pH values are carried out and results are shown in Figure 7. It was observed that the rate of degradation is higher in the acidic pH range (pH = 3.0 and 6.0) than in alkaline pH (pH = 8.0).

The amphoteric behavior of many metal-oxides changes the surface-charge properties of the catalyst when pH changes. For Mg²⁺-TiO₂, increasing the solution pH diminished the adsorption of MO. The zero-point charge pH_{zpc} is 6.25 for TiO₂ particles [34]. In the Mg²⁺-



FT-IR SPECTRAL STUDY

TiO₂ system, TiO₂ is more positively charged in an acidic medium (pH<6.25) than in higher pH, as per the zero-point charge. Hence, at lower pH, MO, which is having electronegative centres (N and O), can have enhanced adsorption on the catalyst surface. This effect acts to increase the degradation of MO at lower pH. All the experiments with different initial pH values were conducted without pH control. It was found that the pH decreased during the photocatalytic degradation of MO.

For instance, the reaction solution with an initial pH 6.0 reached a final pH of 4.5. This drop of the pH indicates the formation of acid products.

Effect of catalyst dosage

Effect of the amount of catalyst on the rate of photodegradation of MO was investigated at a fixed pH and initial concentration of the dye.

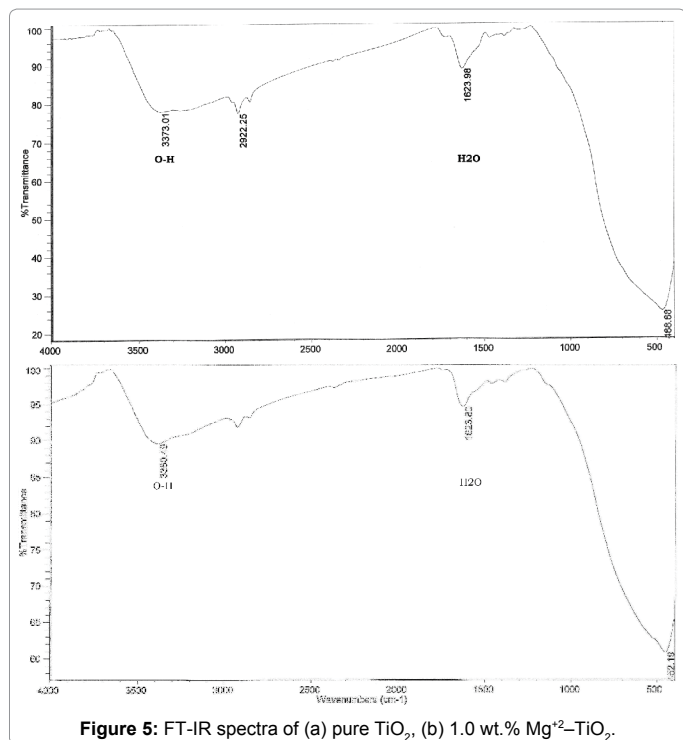


Figure 5: FT-IR spectra of (a) pure TiO₂, (b) 1.0 wt.% Mg²⁺-TiO₂.

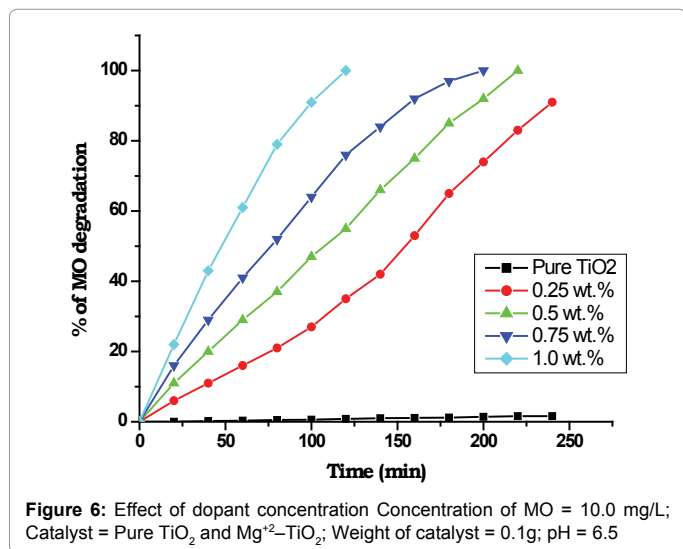


Figure 6: Effect of dopant concentration Concentration of MO = 10.0 mg/L; Catalyst = Pure TiO₂ and Mg²⁺-TiO₂; Weight of catalyst = 0.1g; pH = 6.5

Experiments were performed by varying concentration of Mg²⁺-TiO₂ from 0.1 to 1.1 g in 100 ml of aqueous solution of MO. The degradation results of these experiments have been given in Figure 8. The results reveal that the rate of degradation increases linearly with increase in the amount of catalyst up to 0.7 g, and then decreases (leveling off).

As the amount of catalyst increases, the number of photons and the number of MO molecules adsorbed are increased due to an increase in the number of catalyst particles leading to the increase in photocatalytic efficiency. At higher amounts of catalyst, although more areas are available for constant MO molecules, the number of substrate molecules present in the solution remains the same, but the solution turbidity increases and it interferes the penetration of light and also helps in scattering of radiation. The deactivation of activated molecules by collision with ground state molecules may also hinder

the photocatalytic efficiency [46]. Hence, at a certain level, additional catalyst amount may not involve in catalysis and thus the rate levels off.

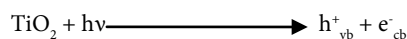
Effect of initial dye concentration

At a fixed concentration of doped TiO₂ and pH, various initial dye concentrations on photocatalytic degradation of MO were studied and the results are presented in Figure 9. It is observed that the rate of degradation increases with increase in dye concentration to 10.0 mg/L and further increase leads to decrease in the rate of degradation. A decrease trend is observed in dye degradation as the dye concentration increases. This may be due to reduction in the generation of •OH radicals on the catalyst surface since the active sites are covered as the dye concentration increases.

Overall mechanism

Based on the experimental results the following mechanism is proposed for the photocatalytic reactions of Mg²⁺-TiO₂.

- i) Upon visible light illumination of photocatalyst, electrons are ejected from the valence band to the conduction band leaving positive holes in the valence band.



- ii) When the metal ion is doped into TiO₂ lattice, these ejected electrons are trapped by dopant ions eliminating the recombination process.



- iii) The trapped electrons can be subsequently scavenged by molecular oxygen, which is adsorbed on the TiO₂ surface, to generate the superoxide radical, and this in turn produce hydrogen peroxide (H₂O₂), hydroperoxy (HO₂•) and hydroxyl (•OH) radicals [47,48].

- iv)

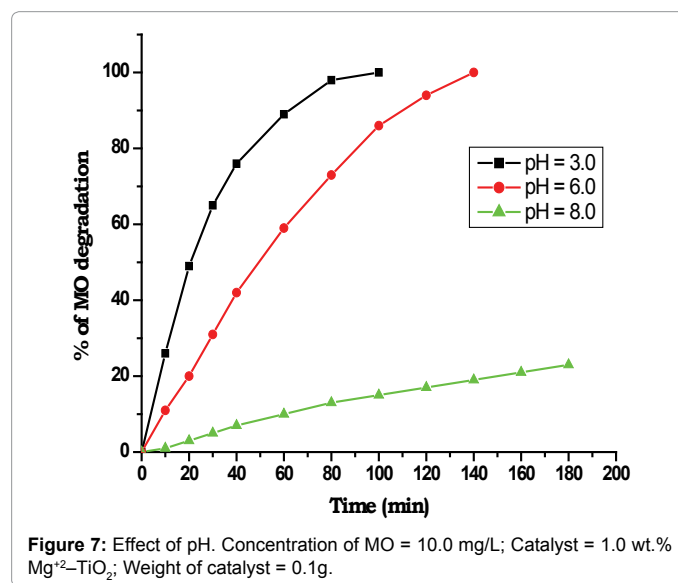
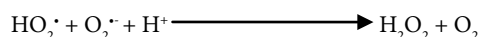


Figure 7: Effect of pH. Concentration of MO = 10.0 mg/L; Catalyst = 1.0 wt.% Mg²⁺-TiO₂; Weight of catalyst = 0.1g.

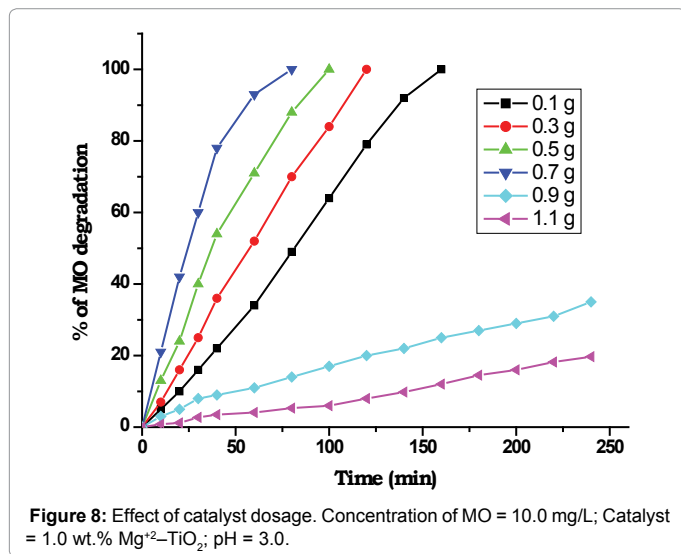


Figure 8: Effect of catalyst dosage. Concentration of MO = 10.0 mg/L; Catalyst = 1.0 wt.% Mg²⁺-TiO₂; pH = 3.0.

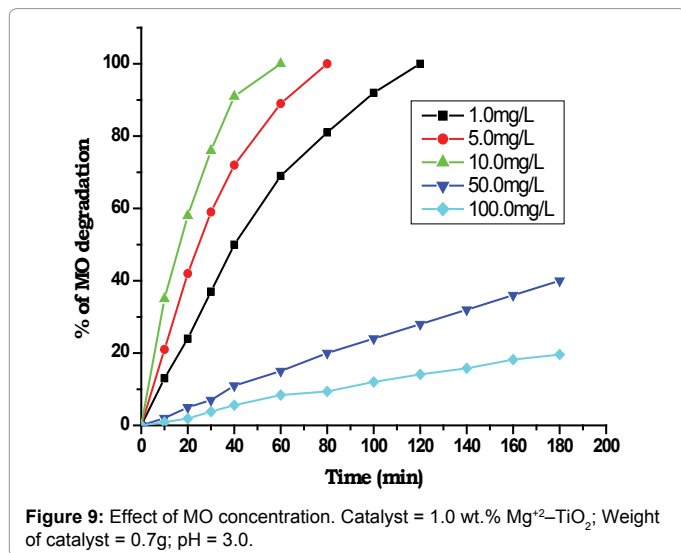


Figure 9: Effect of MO concentration. Catalyst = 1.0 wt.% Mg²⁺-TiO₂; Weight of catalyst = 0.7g; pH = 3.0.



- v) The positive holes in the valence band act as good oxidizing agents available for degradation of pollutants in the solution
- $$\bullet\text{OH} \text{ (or } h^+_{\text{vb}}) + \text{Red} \longrightarrow \text{Red}^+$$

Where 'Red' is the pollutant an electron donor (reductant).

Thus, the pollutant is attacked by the hydroxyl radicals formed both by trapped electrons and hole in the VB as given in the above equations, to generate organic radicals or other intermediates.

During stirring, the dye molecules are adsorbed/desorbed onto the surface of catalyst until the equilibrium formed. Once the solution is illuminated, simultaneously both catalyst and dye get photoactivated. The surface holes of Mg²⁺-TiO₂ photocatalyst consume the dye electrons which are generated by the photosensitization of the dye. In the course of time, metal doped TiO₂ effectively separates the injected electrons and dye cations, thus enhancing the photocatalytic degradation of

adsorbed dye in visible light, than pure TiO₂, Rashed et al. and Bao et al. [49,50] have shown that in case of pure TiO₂ the photodegradation of MO occurred via photosensitization needs more time when compared with the present results. The probable degradation products for methyl orange are acetic acid, water and CO₂ [51,52]. Prospective work can be extended for other azo-dyes attributable on the synthesized Mg²⁺-TiO₂ photocatalyst.

References

- Reid R (1996) Go green – a sound business decision (part I). J Soc Dyers Color 112: 103-105.
- Zollinger H (1991) Color Chemistry: Synthesis, Properties and Applications of Organic Dyes and Pigments, VCH Pubs, New York.
- Nilsson R, Nordlinder R, Wass U, Meding B, Belin L (1993) Asthma, rhinitis, and dermatitis in workers exposed to reactive dyes. Br J Ind Med 50: 65-70.
- Stylidi M, Kondarides DI, Verykios XE (2003) Pathways of solar light-induced photocatalytic degradation of azo dyes in aqueous TiO₂ suspensions. Appl Catal B: Environ 40: 271-286.
- Chung KT, Cerniglia CE (1992) Mutagenicity of azo dyes: structure-activity relationships. Mutat Res 277: 201-220.
- So CM, Cheng MY, Yu JC, Wong PK (2002) Degradation of azo dye Procion Red MX-5B by photocatalytic oxidation. Chemosphere 46: 905-912.
- Turchi CS, Ollis DF (1990) Photocatalytic Degradation of Organic Water Contaminants: Mechanisms Involving Hydroxyl Radical Attack. J Catal 122: 178-192.
- Hoffmann MR, Martin ST, Choi W, Bahnemann DW (1995) Environmental Applications of Semiconductor Photocatalysis. Chem Rev 95: 69-96.
- Legrini O, Oliveros E, Braun AM (1993) Photochemical processes for water treatment. Chem Rev 93: 671-698.
- Ollis DF, Ekabi HA (1993) Photocatalytic Purification and Treatment of Water and Air, Amsterdam 353-494.
- Augustynski J (1993) The role of the surface intermediates in the photoelectrochemical behaviour of anatase and rutile TiO₂. Electrochim Acta 38: 43-46.
- Mills A, Morris S, Davies RH (1993) Photomineralisation of 4-Chlorophenol sensitized by Titanium-dioxide – A study of the intermediates. J Photochem Photobiol A: Chem 70: 183-191.
- Noda H, Oikawa K, Kamada H (1993) ESR spin-trapping study of active oxygen radicals from photoexcited semiconductors in aqueous H₂O₂ solutions. Bull Chem Soc Jpn 66: 455-458.
- Kormann C, Bahnemann DW, Hoffmann MR (1988) Preparation and characterization of quantum-size titanium dioxide. J Phys Chem 92: 5196-5201.
- Linsebigler A, Lu G, Yates JT (1995) Photocatalysis on TiO₂ Surfaces: Principles, mechanisms and selected results. Chem Rev 95: 735-738.
- Bessekhouad Y, Robert D, Weber JV, Chaoui N (2004) Effect of alkaline-doped TiO₂ on photocatalytic efficiency. J Photochem Photobiol A: Chem 167: 49-57.
- Xu AW, Gao Y, Liu HQ (2002) The preparation, characterization and their photo-catalytic activities of rare-earth doped TiO₂ nanoparticles. J Catal 207: 151-157.
- Choi W, Termin A, Hoffmann MR (1994) The role of metal ion dopants in quantum-sized TiO₂: correlation between photoreactivity and charge carrier recombination dynamics. J Phys Chem 98: 13669-13679.
- Xu JC, Shi YL, Huang JE, Wang B, Li HL (2004) Doping metal ions only onto the catalyst surface. J Mol Catal A: Chem 219: 351-355.
- Zhang Z, Wang C, Zakaria R, Ying JY (1998) Role of particle size in nanocrystalline TiO₂-based photocatalysts. J Phys Chem B 102: 10871-10878.
- Sakthivel S, Shankar MV, Palanichamy M, Arabindo B, Bahnemann DW, et al. (2004) Enhancement of photocatalytic activity by metal deposition: characterization and photonic efficiency of Pt, Au and Pd deposited on TiO₂ catalyst. Water Res 38: 3001-3008.
- Lopez T, Hernandez-Ventura R, Gomez R, Tzompantzi F, Sanchez E, et al. (2001) Photodecomposition of 2, 4-dinitroaniline on Li/TiO₂ and Rb/TiO₂ nanocrystallite sol-gel derived catalysts. J Mol Catal A: Chem 167: 101-107.

23. Karakitsou KE, Verykios XE (1993) Effects of alternative cation doping of TiO₂ on its performance as a photocatalyst for water cleavage. *J Phys Chem* 97: 1184-1189.
24. Mu W, Hermann JM, Pichat P (1989) Room temperature photocatalyst oxidation of liquid cyclohexane into cyclohexane over neat and modified TiO₂. *Catal Lett* 3: 73-84.
25. Mazdiyasi KS, Lynch CT, Smith JS (1965) Preparation of ultra-high-purity submicron refractory oxides. *J Am Ceram Soc* 5: 372-375.
26. Barringer EA, Bowen HK (1982) Formation, packing and sintering of monodisperse TiO₂ powders. *J Am Ceram Soc* 65: C-199-C-201.
27. Furlong DN, Parfitt GD (1978) Electrokinetics of titanium dioxide. *J Colloid Interface Sci* 65: 548-554.
28. Duncan JF, Richards RG (1976) Hydrolysis of titanium (IV) sulphate solutions, 2 solution equilibria, kinetics and mechanism. *New Zeal J Sci* 19: 179-183.
29. Cornell RM, Posner AM, Quirk JP (1975) A titrimetric and electrophoretic investigation of the pzc and the iep of pigment rutile. *J Colloid Interface Sci* 53: 6-13.
30. Qian Y, Chen Q, Chen Z, Fan C, Zhou G (1993) Preparation of ultrafine powders of TiO₂ by hydrothermal H₂O₂ oxidation starting from metallic Ti. *J Mater Chem* 3: 203-205.
31. Kim DH, Hong HS, Kim SJ, Song JS, Lee KS (2004) Photocatalytic behaviors and structural characterization of nanocrystalline Fe-doped TiO₂ synthesized by mechanical. *J Alloys and Compounds* 375: 259-264.
32. Ranjit KT, Viswanathan B (1997) Synthesis, characterization and photocatalytic properties of iron-doped TiO₂ catalysts. *J Photochem Photobiol A: Chem* 108: 79-84.
33. Arroyo R, Cordoba G, Padilla J, Lara V (2002) Influence of manganese ions on the anatase-rutile phase transition of TiO₂ prepared by the sol-gel process. *Mater Lett* 54: 397-402.
34. Rengaraj S, Li XZ (2007) Enhanced photocatalytic reduction reaction over Bi(3+)-TiO₂ nanoparticles in presence of formic acid as a hole scavenger. *Chemosphere* 66: 930-938.
35. Kistler SS (1931) Coherent expanded aerogels and jellies. *Nature* 127: 741.
36. Fox MA, Dulay MT (1993) Heterogeneous Photocatalysis. *Chem Rev* 93: 341-357.
37. JCPDS Reference Code: 89-4921.
38. Nair J, Nair P, Mizukami F, Osawa Y, Okubo Y (1999) Microstructure and phase transformation behavior of doped nanostructured titania. *Mater Res Bull* 34: 1275-1290.
39. Rao MV, Rajeshwar KV, Vermerker R, Dubow J (1980) Photosynthetic production of H₂ and H₂O₂ on semiconducting oxide grains in aqueous solutions. *J Phys Chem* 84: 1987-1991.
40. Nishimoto S, Ohtani B, Kajiura H, Kagiya T (1985) Correlation of the crystal structure of Titanium Dioxide prepared from Titanium tetra-2-propoxide with the photocatalytic activity for redox reactions in aqueous propan-2-ol and silver salt solutions. *J Chem Soc Faraday Trans* 81: 61-68.
41. Klionsky DJ, Abdelmohsen K, Abe A, Abedin MJ, Abeliovich H, et al. (2016) Guidelines for the use and interpretation of assays for monitoring autophagy (3rd edition). *Autophagy* 12: 1-222.
42. Yao WF, Wang H, Xu H, Cheng XF, Huang J, et al. (2003) Photocatalytic property of Bismuth Titanate Bi₁₂TiO₂₀ crystal. *Appl Catal A: Gen* 243: 185-190.
43. Li XZ, Li FB, Yang CL, Ge WK (2001) Photocatalytic activity of WO_x - TiO₂ under visible light irradiation. *J Photochem Photobiol A: Chem* 141: 209-217.
44. Moulder JF, Stickle WF, Sobol PE, Bomben KD (1992) Handbook of X-ray Photoelectron Spectroscopy. Perkin-Elmer, Eden Prairie.
45. Serpone N, Lawless D (1994) Spectroscopic, photoconductivity, and photocatalytic studies of TiO₂ colloids: naked and with the lattice doped with Cr³⁺, Fe³⁺ and V⁵⁺ cations. *Langmuir* 10: 643-652.
46. Shannon RD (1976) Revised effective ionic radii and systematic studies of interatomic distances in halides and chalcogenides. *Acta Cryst A* 32: 751-767.
47. Neppolian B, Choi HC, Sakthivel S, Arabindoo B, Murugesan V (2002) Solar/UV-induced photocatalytic degradation of three commercial textile dyes. *J Hazard Mater* 89: 303-317.
48. Wu T, Liu G, Zhao J, Hidaka H, Serpone N (1999) Evidence for H₂O₂ generation during the TiO₂-assisted photodegradation of dyes in aqueous dispersions under visible light illumination. *J Phys Chem B* 103: 4862-4867.
49. Wu T, Liu G, Zhao J, Hidaka H, Serpone N (1999) TiO₂-assisted photodegradation of dyes. 9. Photooxidation of a squarylium cyanine dye in aqueous dispersion under visible light irradiation. *Environ Sci Tech Lett* 33: 1379-1387.
50. Rashed MN, El-Amin AA (2007) Photocatalytic degradation of methyl orange in aqueous TiO₂ under different solar irradiation sources. *Int J Phys Sci* 2: 073-081.
51. Bao X, Yan SS, Chen F, Zhang J (2005) Preparation of TiO₂ photocatalyst by hydrothermal method from aqueous peroxy titanium acid gel. *Mater Lett* 59: 412-415.
52. Jianying G, Weimin C (2007) Degradation of methyl orange in water by contact glow discharge electrolysis. *Plasma Sci Technol* 9: 190-193.